

# Development of a Digital Laser Offset Lock System

A thesis submitted in partial fulfillment of requirements for the degree of Bachelor of Science in Physics from the College of William and Mary in Virginia.

by  
Lauren Snowden White

Advisor: Seth Aubin  
Senior Research Coordinator: Henry Krakauer

Williamsburg, Virginia  
7 May 2012

## **Abstract**

This thesis describes the development of a laser locking system used to stabilize the optical frequency of an unstable laser relative to a second, stable control laser. Directing these two lasers onto a photodetector produces a difference in the two optical laser frequencies called a beat note. The laser lock electronics analyze the beat note frequency and use feedback to the slaver laser to stabilize it relative to the master laser. When the laser lock system is completed, it will be used to tune a titanium- sapphire laser in the College of William and Mary's Ultra-cold Atomic, Molecular and Optical (AMO) physics laboratory. The digital optical frequency offset lock can also be used to lock lasers for experiments exploring two-level and three-level atomic systems.

## **1 Introduction**

This thesis describes a project to design an optoelectronic system that can lock the frequency of the electric field oscillations of the light field of one laser to another. At high optical frequency differences, specifically in the range of GHz, there exists a need for an inexpensive electronic system to stabilize relative laser frequencies. This system can be useful in many experiments involving light and matter interactions [1]. For this project, the system, called an optical frequency lock loop (OFLL), will be used in the Ultra-cold AMO physics laboratory at the College of William and Mary to lock a titanium-sapphire laser's frequency to a stable diode laser's frequency. Both of these lasers have an approximate frequency of  $3.85 \times 10^{14}$  Hz, but the titanium-sapphire laser's frequency is fluctuating in the MHz range and drifting in the 0-100 MHz range. While an analog laser lock system has already been built for the Ultra-cold AMO physics laboratory, a higher quality lock on the frequency difference between the titanium-sapphire laser and diode laser is needed.

A digital laser lock may be used in many different systems where having a fixed optical frequency difference is integral to its function. The addition of a frequency locked titanium-sapphire laser to the Magneto Optical Trap (MOT) in the AMO physics laboratory will increase the number of trapped ultracold atoms. The added laser must have the same frequency of electric field oscillations of the light field as the lasers already in place. The OFLL will be used to lock these lasers. Some experiments require a high magnetic field, which causes the energy separation between the ground and first optically excited states of trapped atoms to increase due to the Zeeman shift. In these experiments, an additional laser with the ability to target these atoms is necessary [2]. A digital laser lock has the flexibility to lock an additional laser to the appropriate optical frequency required for operation at high magnetic field.

In three-level systems, atoms in one ground level  $g_1$  can be transferred coherently to another ground level  $g_2$  through Stimulated RAMAN Adiabatic Passage (STIRAP) by applying two laser fields that connect the two ground levels with a common excited state [3]. A high quality laser lock system is required to stabilize the frequency difference between the two lasers. Furthermore, when two frequency offset locked lasers are tuned to interact with the excited and two ground states in a specific way, destructive interference occurs, transforming a previously impenetrable atomic medium into a transparent one. While a single laser with frequency  $\omega_1$  would be absorbed by the medium, the addition of a second laser with frequency  $\omega_2$  cancels the absorption of  $\omega_1$  in a phenomenon referred to as electromagnetically induced transparency (EIT) [4]. Without the lasers' frequencies being precisely locked, this phenomenon would not occur. Four-wave mixing, the use of two lasers incident on a medium to produce a third laser of

different frequency through a nonlinear optical process, also requires the system's lasers to be precisely locked [5].

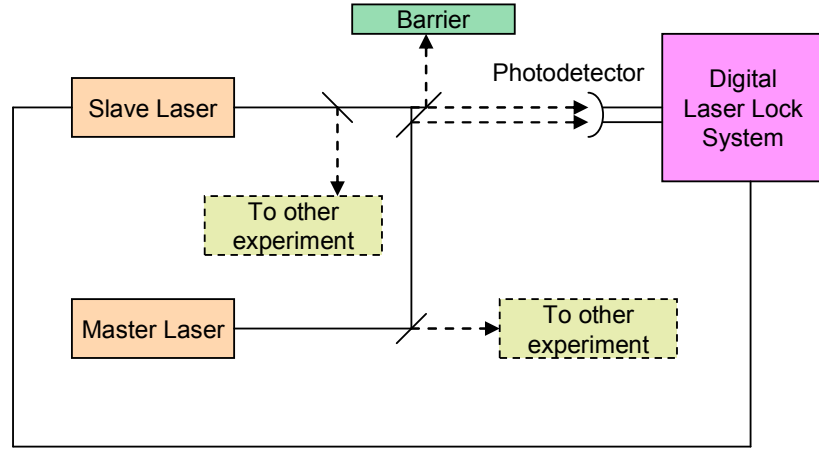


Figure 1: Basic schematic for the digital laser lock system including an unstable (slave) laser, a stable (master), an optical detector (photodetector) where the incident optical signal is transformed to an electrical signal, and a loop filter within the digital laser lock system which adjusts the optical signal.

The OFLL basic design shown in Figure 1 includes two lasers, an unstable laser and a stable laser, referred to as the slave and master lasers respectively, an optical detector to transform the optical signal into an electrical signal, and a loop filter which analyzes and gradually corrects the slave laser's optical frequency. While the laser lock system has many important parts, the photodetector is the integral step between optics and electronics. It detects the power of the incident beam, which is given by

$$\langle I \rangle = \frac{1}{2} c \epsilon_0 E^2 [\cos^2(\omega_1 t + \phi_1) + \cos^2(\omega_2 t + \phi_2) + 2 \cos(\omega_1 t + \phi_1) \cos(\omega_2 t + \phi_2)], \quad (1)$$

where  $E$  is electric field amplitude assumed to be identical for both lasers,  $\epsilon_0$  is the permittivity of free space,  $t$  is time,  $\omega_1$  is the frequency of the slave laser that is being tuned,  $\phi_1$  is its phase,  $\omega_2$  is the frequency of the master laser that is being used as a control,  $\phi_2$  is its phase, and  $c$  is the speed of light. The frequencies of the two lasers,

described in part by the  $\cos^2(\omega_1 t + \phi_1)$  and  $\cos^2(\omega_2 t + \phi_2)$  terms, are each too fast for existing electronics to recognize, as they are optical frequencies oscillating in the range of  $10^{14}$  Hz. For this reason, both terms average to  $\frac{1}{2}$ , and equation (1) is simplified to

$$\langle I \rangle = \frac{1}{2} c \epsilon_0 E^2 \left[ \left( \frac{1}{2} \right) + \left( \frac{1}{2} \right) + 2 \cos(\omega_1 t + \phi_1) \cos(\omega_2 t + \phi_2) \right], \quad (2)$$

Using the trigonometric identity  $\cos(x) \cos(y) = \frac{1}{2} [\cos(x - y) + \cos(x + y)]$  to expand the second term and consolidating the first two terms, equation (2) becomes

$$\langle I \rangle = \frac{1}{2} c \epsilon_0 E^2 \{ 1 + \cos[(\omega_1 - \omega_2)t + \phi_1 - \phi_2] + \cos[(\omega_1 + \omega_2)t + \phi_1 + \phi_2] \} \quad (3)$$

With the knowledge that  $\cos[(\omega_1 + \omega_2)t + \phi_1 + \phi_2]$  averages to zero because  $\omega_1$  and  $\omega_2$  are optical frequencies oscillating too quickly for existing electronics, equation (3) reduces to

$$\langle I \rangle = \frac{1}{2} c \epsilon_0 E^2 \{ 1 + \cos[(\omega_1 - \omega_2)t + \phi_1 - \phi_2] \}, \quad (4)$$

where the cosine term defines the beat note oscillations at up to  $\sim 10$  GHz that the photodetector in this laser lock system measures [7]. The aim of the laser lock system is to lock  $\Delta \omega = \omega_1 - \omega_2$  equal to a constant frequency difference.  $\Delta \omega$  is called the beat note and typically oscillates in the GHz range.

## 2 Design and Implementation

The design in Figure 2 shows the schematic for the digital laser lock system being built for this project [6]. In addition to the master and slave laser and photodetector described above and shown in Figure 1, the detailed diagram of the loop filter, or digital laser lock system, provides a more clear sense of its specific function. The system includes a limiting amplifier, high frequency divider, low-noise amplifier, and another

amplifier that all increase the signal for analysis by a field-programmable gate array (FPGA). The FPGA produces a digital error signal that is converted back to an analog signal in order to modulate the slave laser's optical frequency.

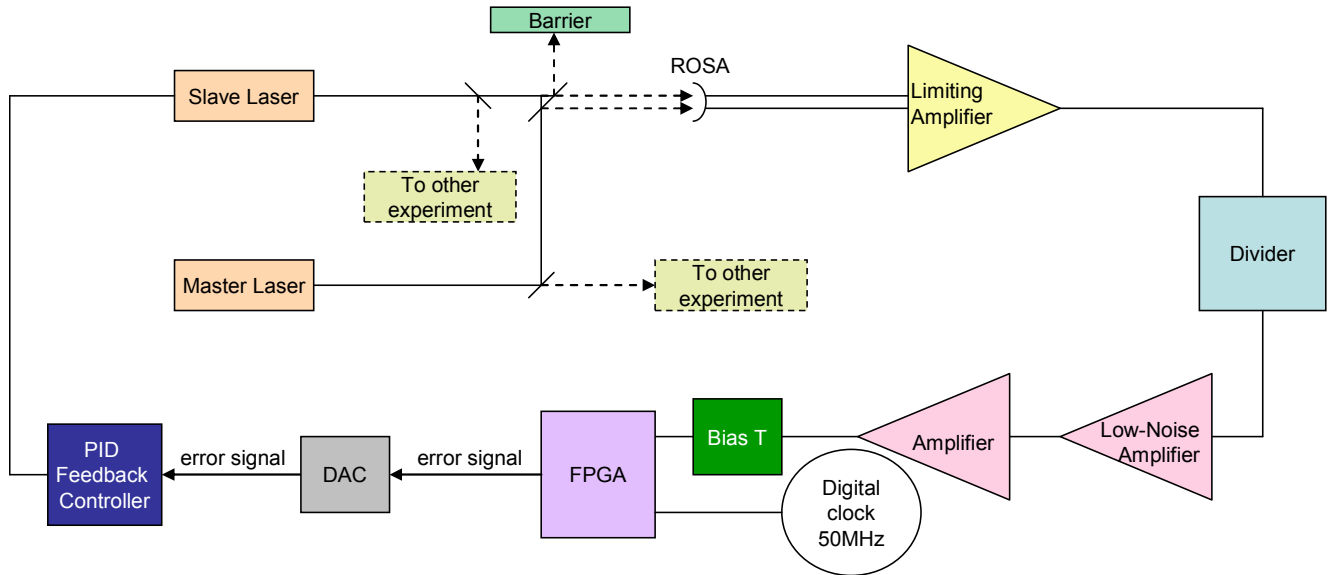
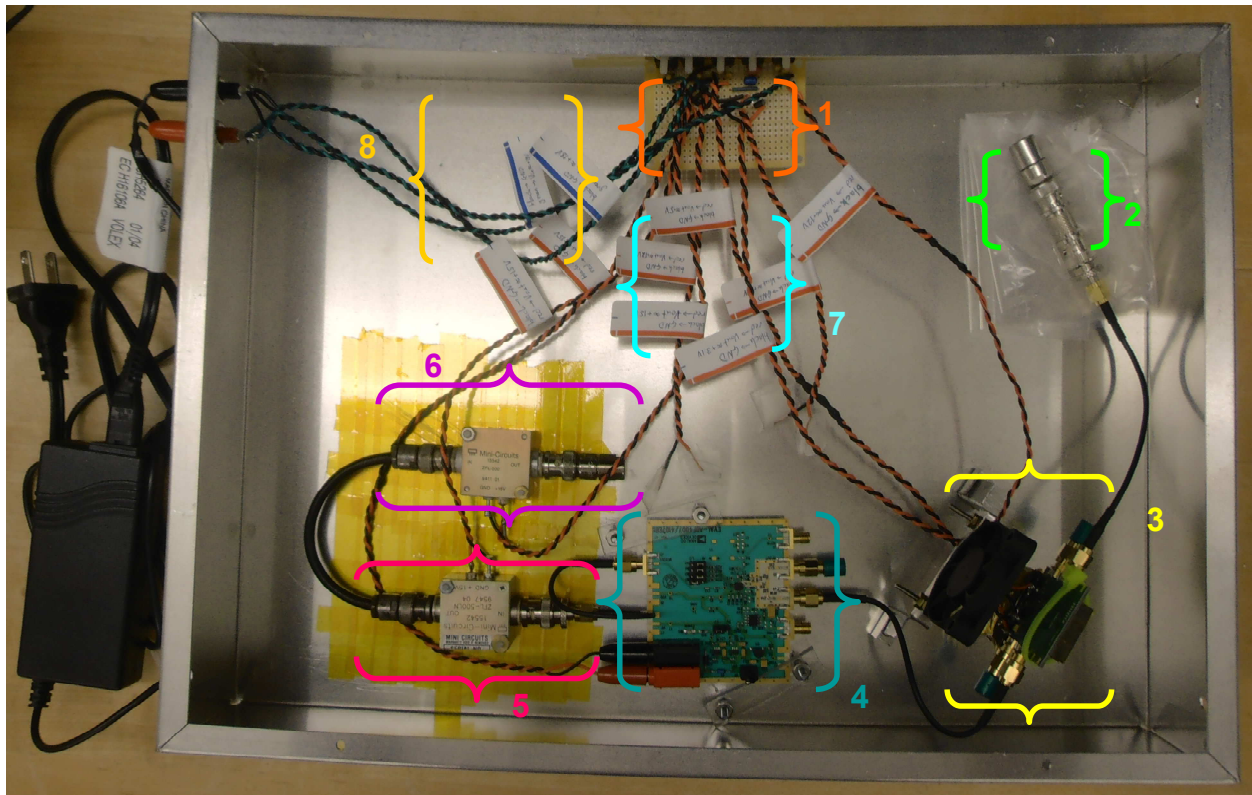


Figure 2: Schematic for digital laser lock system. The optical signal from the slave and master lasers enter the laser lock through an optical fiber and onto the Receiver Optical Sub-Assembly (ROSA) photodetector which produces an electrical signal that is amplified into a square wave by the limiting amplifier. This frequency is reduced by a factor of 8, 16, 32, or 64 by the divider. The signal is then amplified by two amplifiers, shifted to oscillate above zero by the Bias T, and counted, analyzed, and modified by the FPGA-Digital clock combination. The digital error signal is converted back to an analog signal by the digital-to-analog converter (DAC), and tuned by the proportional–integral–derivative (PID) feedback controller. This feedback process is repeated until  $\Delta\omega$  is fixed.

One of the primary tasks of electrical circuit construction is testing. While installing components into the aluminum enclosure may prove to be a spatial challenge, it is most important to test each component of the circuit as each part is installed, or else the challenge of finding the source of a problem later may prove quite trying. Each of the components that have been installed into the aluminum enclosure thus far (see Figure 3)

have been tested for general operation as well as for the specific function required for the laser lock circuit.

When creating a circuit, especially one with high frequency components, the enclosure in which the circuit is being constructed as well as those working on construction of the circuit must be grounded. This is to avoid any damage to the circuit due to static electricity. In the laser lock system, each part that is added to the aluminum enclosure must be securely attached so as not to move, while leaving enough room to attach and detach wires, and must also be insulated so no metal components are in contact with the metal box. This would essentially ground the entire circuit to the enclosure.



*Figure 3: Image of laser lock system thus far in aluminum enclosure. 1. Power supply; 2. Optical detection system including ROSA (not yet present); 3. Limiting Amplifier and cooling fan; 4. Divider; 5. Low Noise Amplifier; 6. Amplifier and Bias T (not yet present); 7. FPGA with 50MHz Digital Clock (not yet installed); 8. DAC and PID Feedback Controller (not yet present).*

## 2.a Power Supply

Each element of the system has a required voltage with which it must be powered. Regulators are used to produce a series of power supply voltages, shown in the table of Figure 4, from one main 18V source. These voltages are then connected with a common ground to each element of the system. The power supply board, which is indicated with a 1 in Figure 3, was the first part of the system built. Each of the main circuit parts requires a different power supply voltage. Stranded wire was used to connect the power supply board to each of the circuit parts. Each of the wires carrying voltage is twisted with a ground wire to reduce the electromagnetic interference present when using high frequency signals [8].

<b>Circuit Part</b>	ROSA	Limiting Amplifier (HMC750LP4)	Divider (ADF4007)	Amplifier (ZFL-500LN)	Amplifier (ZFL-500)	FPGA
<b>Voltage Required</b>	+3.3	+5.0	+15.0	+15.0	+15.0	+9.0

*Figure 4: Required voltage for the basic elements of the OFLL within the enclosure.*

## 2.b Optical Detection System

The OFLL begins with the slave laser and master laser. Using optical lenses to focus the two laser beams into a parallel path, the beams are directed onto an optical receiving lens. The incident intensity on the optical receiving lens is transmitted through an optical fiber to the Receiver Optical Sub-Assembly (ROSA) where the beat note is converted to an electronic signal. This electronic signal will be used in the digital laser lock system to slightly alter the optical frequency of the slave laser with each iteration of the optical frequency-locked-loop (OFLL) until the beat note is held fixed [1].



The ROSA will be mounted in the enclosure in the space indicated with a 2 in Figure 3 after testing. A distinctly secure mount has been created for the optical receiving lens, and the optical fiber has been attached to the optical receiving lens. The electronic signal will travel from the ROSA to the limiting amplifier in a short SMA cable.

## **2.c Limiting Amplifier**

From the ROSA the signal travels to the limiting amplifier (Hittite Microwave Corporation HMC750LP4). Here the signal is significantly amplified and converted to a digital square wave. From this point in the OFLL, the system will operate with a square wave signal. The limiting amplifier, indicated with a number 3 in Figure 3, was installed vertically in the aluminum enclosure using an aluminum mount covered in insulating tape and a zip-tie with double-sided tape to secure it to the mount. Four place-holding  $0\Omega$  resistors that were surface mounted to the limiting amplifier were causing significant temperature increase that could damage the limiting amplifier. To amend this, these four resistors were removed and replaced with four  $0.1\mu\text{F}$  surface mount capacitors to AC-couple the signal to the limiting amplifier. The main chip in the limiting amplifier circuit was still reaching a borderline worrisome temperature, so a fan was mounted in the enclosure to cool the chip, which resolved the heating problem.

Because the limiting amplifier was one of the more recently installed pieces of the circuit, many variables came into play when testing it. When compared to the data plots previously collected when testing the high frequency divider and the two amplifiers, the limiting amplifier amplifies the signal  $\sim 5x$  as well as clearly tuning the shape to more of a square wave, as can be seen in Figure 5. It was found that a higher division by the high

frequency divider and a higher input frequency into the limiting amplifier produced higher output amplitudes at smaller power levels, as can be seen in Figure 6.

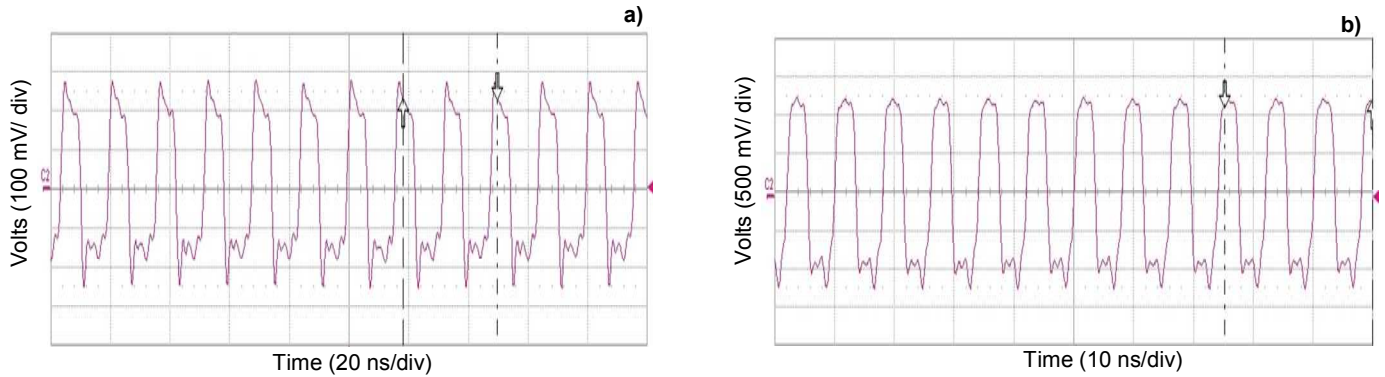


Figure 5: Data plots of input frequency (1000MHz) into a) high frequency divider (divide-by-8) and two amplifiers b) limiting amplifier, high frequency divider (divide-by-8), and two amplifiers at -37.2 dBm. Signal shaped more closely to a square wave and amplified ~5x with the limiting amplifier.

%	Frequency (MHz)	Limit of signal
8	500	-34.4 dBm @ 2000 MHz
8	1000	-37.2 dBm @ 2250 MHz
8	1500	-37.5 dBm @ 2000 MHz
8	2000	-38.9 dBm @ 2000 MHz
16	500	-34.4 dBm @ 2500 MHz
16	1000	-37.2 dBm @ 2000 MHz
16	1500	-37.4 dBm @ 2250 MHz
16	2000	-39.2 dBm @ 2250 MHz
32	500	-34.2 dBm @ 2500 MHz
32	1000	-37.4 dBm @ 2500 MHz
32	1500	-37.6 dBm @ 2250 MHz
32	2000	-39.3 dBm @ 2250 MHz
64	500	-33.9 dBm @ 2500 MHz
64	1000	-37.1 dBm @ 2500 MHz
64	1500	-37.6 dBm @ 2500 MHz
64	2000	-39.6 dBm @ 2500 MHz

Figure 6: Test results of input frequency (MHz) into limiting amplifier and output frequency after traveling through high frequency divider and two amplifiers. Higher divisions produce higher output voltages as well as larger power levels.

## 2.d High Frequency Divider

The signal from the limiting amplifier is next passed through a high frequency divider (Analog Devices ADF4007). A low noise divider is used to divide the frequency of the square wave by 8, 16, 32, or 64 depending on how the system's N counter is set. Following the construction and installation of the power supply board, the high frequency divider was mounted into the enclosure, which can be seen in Figure 3 as object 4. Using an oscilloscope and function generator, the divider was tested for its input bandwidth at each of the divide by 8, 16, 32 and 64 settings. When doing initial set-up for testing, it was discovered that the power switch on the high frequency divider is installed backward by the manufacturer. Because the signal generator used for testing the high frequency divider has an upper limit of 2 GHz, only the input bandwidth lower limit for each setting, listed in Figure 7, could be found. Results showed distortion in the oscillations at random frequency intervals as well as a lack of the large desired amplitude, as can be seen in Figure 8a, an oscilloscope display capture from testing.

<b>Divider Settings</b>	<b>8</b>	<b>16</b>	<b>32</b>	<b>64</b>
<b>Frequency Bandwidth Lower Limit of Divider (MHz)</b>	169	250	500	500
<b>Frequency Bandwidth Lower Limit of Divider with Low Noise Amplifier (MHz)</b>	155	160	150	256
<b>Frequency Bandwidth Lower Limit of Divider with Low Noise and standard Amplifier (MHz)</b>	159	160	154	255

*Figure 7: Bandwidth lower limit for divider without amplifiers, with divider and low noise amplifier in series, and with divider, low noise amplifier and a second amplifier in series. Lower limit gradually increases with “divide by” setting changed from 8 to 64 but tends to decrease with the addition of amplifiers.*

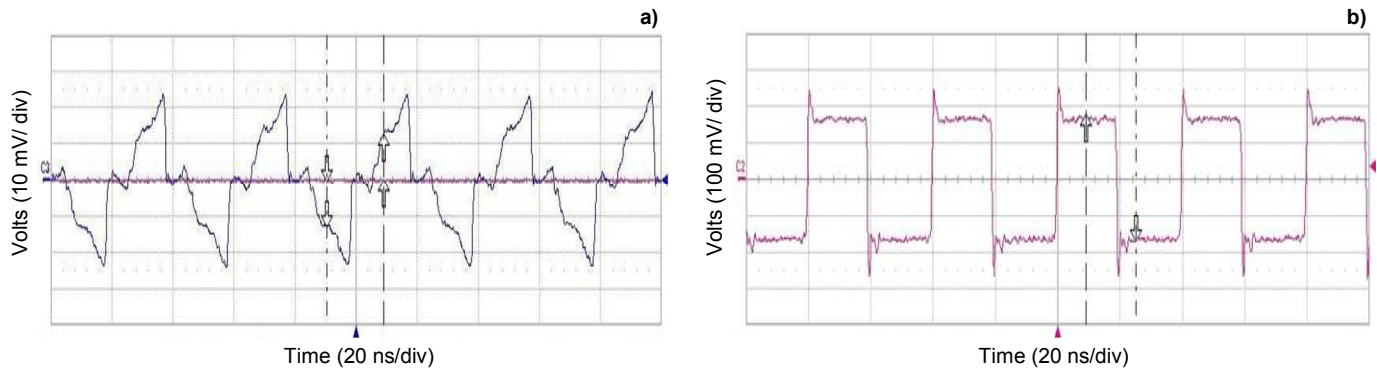


Figure 8: a) Oscilloscope display capture from testing divider alone at frequency of 800MHz with +4.5dBm input signal power and divide by 32 setting on high frequency divider. Shows distortion in the oscillations as well as a lack of the large amplitude desired. b) Oscilloscope display capture from testing divider with low noise amplifier at frequency of 800MHz with +4.5dBm input signal power and divide by 32 setting on high frequency divider. Shows fixed distortion in oscillations and some enlargement of amplitude.

## 2.e Amplifiers and Bias T

To decrease distortion in the signal as well as increase the amplitude of oscillation, the divided signal then travels through a low noise amplifier (Mini-Circuits ZFL-500LN), as can be seen in Figure 3 as object 5. Again using an oscilloscope and signal generator, the low noise amplifier was tested for its bandwidth at each of the divide by 8, 16, 32 and 64 settings. As before, only the bandwidth lower limit could be found, as seen in Figure 7. The output signal was between  $\sim 5x$  and  $\sim 20x$  the size of the input signal coming from the divider and shows significantly less distortion, as is seen in Figure 8b.

Because adding one amplifier worked so well, the next step was to add a second amplifier (Mini-Circuits ZFL-500) following the low noise amplifier in series to amplify the signal sufficiently for use with the Field-Programmable Gate Array (FPGA). The first amplifier's low noise characteristic limits its ability to amplify the signal. The second amplifier may have associated noise, but it produces a robust signal that is well

matched with the voltage levels at the FPGA. Using an oscilloscope and function generator, the second amplifier was tested for its lower bandwidth limit at each of the divide by 8, 16, 32, and 64 settings, as seen in Figure 7.

The output signal from the second amplifier is likely to oscillate around zero. For the FPGA to properly detect the signal, the oscillations must all be positive. In the case that the output signal from the second amplifier does oscillate around zero, a Bias T will be installed after the second amplifier to shift the signal into the positive region for further analysis.

## **2.f FPGA and 50MHz Digital Clock**

From the second amplifier, the signal goes to an FPGA-based digital counter, which will be installed in the enclosure in the space denoted with a 7 in Figure 3. A Terasic DE0 development board is equipped with an Altera Cyclone III EP3C16F484 FPGA that is programmed (Verilog) to compare a beat note frequency counter with a control counter using a 50MHz internal digital clock as a controlled timer. As the clock runs, it counts the specific number of oscillations expected if the two lasers are locked to a beat note  $\Delta\omega$  during an allotted amount of time.

When determining what this number would be for this OFLL, length of count time and accuracy had to be balanced. The longer the count time, the more accurate the loop filter would be, but it would also take so long it would be inefficient at correcting transients. Taking these two factors into account and assuming an input signal of  $\sim 7$  GHz using the high frequency divider's divide-by-64 function, a target error signal of 1 MHz or less was chosen. The ratio between the input signal and error signal was taken to determine that the “stop count” number should be  $\sim 10^4$  or higher, more specifically a

number of  $2^{14}$  or higher, as a lower “stop count” number would increase the error. The period would be 20ns for a 50 MHz clock, which, when multiplied by the “stop count” number  $2^{14}$ , translates to a count time of  $\sim 328\mu\text{s}$ . Because this is not a very long count time, it was decided to increase the value by adding an extra bit to the binary count number to account for error. This produced a “stop count” number of  $2^{16}-1$  with a corresponding count time of  $\sim 1.3\text{ms}$  to increase efficiency of correcting transients.

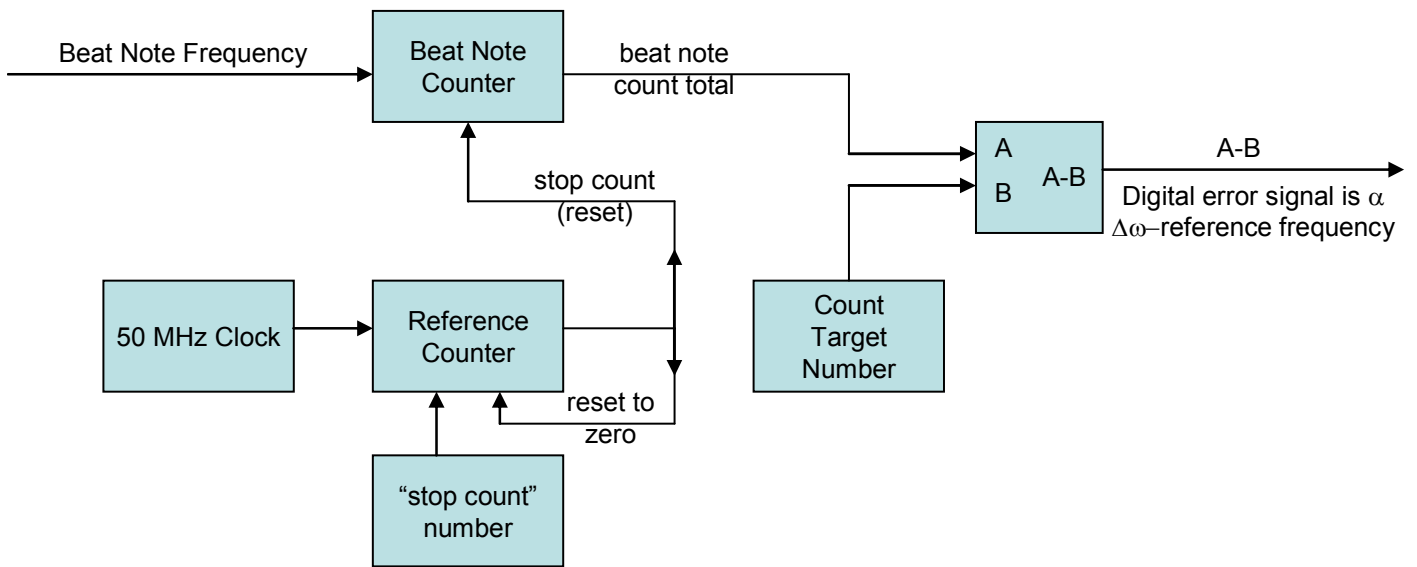


Figure 9: Basic schematic for FPGA program written in Verilog to count beat note frequency and time it relative to a reference frequency provided by an internal 50 MHz Clock. The difference between the beat note frequency and an inputted count target number is the output error signal.

Each time the reference counter reaches  $2^{16}$ , it is triggered to stop counting and to make the control counter stop counting as well. Both counters reset to zero to begin counting again and the beat note counter total is compared to a count target number. The count target number will be set to expect a specific number of oscillations per unit time. If more oscillations are incident on the beat note counter than the reference counter in the allotted time, the frequency is too high. If fewer oscillations are incident on the beat note

counter than the reference counter in the allotted time, the frequency is too low. This process will ultimately output the difference between the count target number and the beat note counter total as the error signal. This basic set-up can be seen in Figure 9 (see Appendix for full source code).

## **2.g DAC and Feedback Controller**

The digital error signal from the FPGA must be converted back to an analog signal using a Digital-to-Analog Converter (DAC). This analog error signal is sent to the Proportional-Integral-Derivative (PID) feedback controller. This is where the signal will be stabilized and fine tuned to be transmitted to the slave laser. The signal will continue to travel this optical frequency-locked-loop (OFLL) and be corrected until  $\Delta\omega$ , the beat note, is constant [1]. The DAC and PID feedback controller will be installed into the aluminum enclosure in the area marked 8 in Figure 3. Once these pieces have been constructed and installed, the remainder of the construction process will consist of fine tuning the system for optimal performance.

## **3 Conclusions**

While the College of William and Mary's Ultra-cold AMO physics laboratory already has an analog laser lock system, the digital laser lock system has some advantages. Analog devices tend to work more quickly and with a lower noise level than digital devices; however the output range of analog phase frequency difference detector is limited. A digital system allows the user to tailor the gain of the feedback over a wide range of feedback rates whereas the feedback of an analog lock system is fixed [7].

Because this design for a digital laser lock system is a combination of analog and digital systems, the circuit will work more quickly while producing less noise than would an all-digital system.

While this digital laser offset lock system has many components, the majority of the loop filter's work is done within the FPGA. The core program presently in use is relatively basic. When this system is next upgraded, a feature may be added such that when a count target number is provided in binary through setting external switches high and low, that number will be inserted into the core FPGA program. Another option would be adding a target count number calculator that will compute and update the desired target count number based on information provided through external switches and the first iteration of the loop filter. Adding multiple loop filters with different count times to the core code would be an upgrade that would make the system more accurate as it would accommodate the benefits of both the increased accuracy of longer count times and the efficiency of shorter count times.

The ROSA and its associated circuit have been assembled by Megan Ivory, however its functionality must still be tested. Once the ROSA is confirmed to work, it will be installed in the aluminum enclosure in the area marked with a 2 in Figure 3. The DAC and PID feedback controller need to be assembled and installed along with the FPGA, which has already been tested independently. Testing of the fully assembled system will determine if a Bias T is necessary. The laser lock will then be applied to the unstable titanium-sapphire laser or an unlocked diode laser with a stable diode master laser as a control in the Ultra-cold AMO laboratory.



## Appendix

*Listing 1: Quartus code for FPGA counter used to stabilize slave laser relative to master laser.*

```
////////////////////////////////////
// Fix the electronic beat note between 50MHz clock and input electronic signal.
// Last modified by Lauren Snowden White 7 May 2012.
////////////////////////////////////

module counter101(input1,input2,output1,output1_display);
    input input1; // reference clock input to reference counter
                      // 50 MHz internal clock
    input input2; // beat note frequency input to beat note counter
    output output1; // reference clock output; used for coding
    output [15:0] output1_display; // beat note counter output, 16 bits binary
    reg [15:0] counttime_test_in;
    // beat note input counter, gives number of counts/1.3ms, 16 bits binary
    reg [15:0] counttime_test_out; // beat note output counter, 16 bits binary
    // gives number of counts/1.3ms counted by counttime_test_in
    reg [15:0] counttime_ref;
    // reference clock counter gives number of counts/1.3ms, 16 bits binary
    reg ref_count_complete;
    // reference clock counter has completed count to 1.3ms, 1 bit binary
    // (2^(16)-1 = 65,535 oscillations)
    initial
        begin
            counttime_test_in = 16'b0000000000000000;
            // set beat note clock input counter to zero
            counttime_test_out = 16'b0000000000000000;
            // set beat note clock output counter to zero
            counttime_ref = 16'b0000000000000000;
            // set reference 50 MHz clock count time to zero
            ref_count_complete = 1'b0;
            // indicate that reference clock counter should count normally
        end

    assign output1_display [15:0] = counttime_test_out [15:0];
    // attach so beat note count total is sent to output display
    always@ (posedge input1) // begin at low to high transition of 50 MHz clock
        begin
            counttime_ref <= counttime_ref + 16'b0000000000000001;
            // counting of reference 50 MHz clock begins
            ref_count_complete = 1'b0;
            // reference clock counter set low so will count normally
            if (counttime_ref == 16'b1111111111111111)
                // "stop count" # =65,535 beats of reference clock = 1111111111111111
                begin
                    counttime_test_out <= counttime_test_in;
                    // counttime_test_out gives the number of counts counted by
                    // counttime_test_in in 1.3ms
                    counttime_ref <= 16'b0000000000000000;
                    // reset reference count time to zero
                    ref_count_complete <= 1'b1;
                    // set high to indicate temp counter is full
                end
        end
end
```

```

always@ (posedge input2 or posedge ref_count_complete)
// begin at low to high transition of beat note signal
// or begin at low to high transition of complete reference count indicator
begin
    if (ref_count_complete == 1'b1) // if reference counter flag high
        begin
            counttime_test_in <= 16'b0000000000000000;
            // reset input beat note counter to zero
        end
    else
        begin
            counttime_test_in <= counttime_test_in + 16'b0000000000000001;
            // begin counting of beat note again
        end
    end
endmodule

```

## Acknowledgements

I would like to thank Professor Aubin for his direction and dedicated support on this project. I would also like to thank Megan Ivory, Austin Ziltz, and Alexander (Sandro) Gvakharia for any and all suggestions and assistance given to me on this project.

## References

- [1] J. Appel, A. MacRae, and A.I. Lvovsky, Meas. Sci. Technol. 20, 055302 (5pp) (2009); (10.1088/0957-0233/20/5/055302).
- [2] U. Ernst, A. Marte, F. Schreck, J. Schuster, and G. Rempe, Europhysics Letters 41 (1), pp. 1-6 (1998).
- [3] K.-K. Ni, S. Ospelkaus, M. H. G. de Miranda, A. Pe'er, B. Neyenhuis, J. J. Zirbel, S. Kotochigova, P. S. Julianne, D. S. Jin, and J. Ye, Science 322, 231 (2008); published online 18 September 2008 (10.1126/science.1163861).
- [4] L. V. Hau, S. E. Harris, Z. Dutton, and C. H. Behroozi, Nature 397, 594-598 (1998); published online 18 February 1999 (10.1038/17561).
- [5] R. C. Pooser, A. M. Marino, V. Boyer, K. M. Jones, and P. D. Lett, 2009, Quantum correlated light beams from nondegenerate four-wave mixing in an atomic vapor: the D1 and D2 lines of  $^{85}\text{Rb}$  and  $^{87}\text{Rb}$ , *Optical Society of America*.
- [6] A. M. Marino and C. R. Stroud, Jr., Rev. Sci. Instrum. 79, 013104 (2007); published online 11 January 2008 (10.1063/1.2823330).
- [7] L. Cacciapuoti, M. de Angelis, M. Fattori, G. Lamporesi, T. Petelski, M. Prevedelli, J. Stuhler, and G. M. Tino, Rev. Sci. Instrum. 76, 053111 (2005); published online 2 May 2005 (10.1063/1.1914785).
- [8] R. Getz and B. Moeckel, 1996, Understanding and Eliminating EMI in Microcontroller Applications, *National Semiconductor Corporation*, p.13.